



*Original Article*

## Influence of compaction pressure on the morphology and phase evolution of porous NiTi alloy prepared by SHS technique

Sirikul Wisutmethangoon<sup>1</sup>, Nipon Denmud<sup>2</sup>, Lek Sikong<sup>2</sup> and Weerawan Suttisripok<sup>2</sup>

<sup>1</sup>*Department of Mechanical Engineering,*

<sup>2</sup>*Department of Mining and Materials Engineering, Faculty of Engineering,  
Prince of Songkla University, Hat Yai, Songkhla, 90112 Thailand.*

Received 4 March 2008; Accepted 14 August 2008

---

### Abstract

The influence of compaction pressure on the pore morphology of porous NiTi shape memory alloys (SMAs) fabricated by self-propagating high-temperature synthesis (SHS) was investigated. The compaction pressure has a significant effect on the combustion temperature and pore morphology. The porous NiTi (SMAs) thus obtained have the porosity of product in the range of 37.4-57.9 vol.%. The open porosity ratios were observed to be greater than 88%, which indicates that porous NiTi (SMAs) are suitable for biomedical applications. In addition, the predominant phases in the porous product are B2(NiTi) and B19'(NiTi) with small amounts of secondary phases, NiTi<sub>2</sub> and Ni<sub>4</sub>Ti<sub>3</sub>.

**Keywords:** shape memory alloy, combustion synthesis, self-propagating high temperature synthesis, porous materials

---

### 1. Introduction

Combustion synthesis (CS) or self-propagating high temperature synthesis (SHS) can be effectively used for the production of powder and porous bodies of intermetallic compounds and ceramics. The synthesis reaction occurs generally through ignition, propagation of combustion wave front and cooling. Various heat sources used to ignite samples are, for instance, tungsten coil (Yeh and Sung., 2004), electric arc, electrically heated Mo filament, a magnesium ribbon, laser pulse (Bertolino *et al.*, 2003), highly exothermic reaction, rapid heating in a furnace, or microwave energy (Ganesh *et al.*, 2005). Combustion reaction can be induced either by a self-propagating mode or by a thermal explosion mode. The process with the advantages of time and energy savings has been recognized as an attractive alternative to the conventional methods of producing advanced materials, such as carbides, borides, nitrides, hydrides, and

intermetallics, etc. (Yeh and Sung., 2004).

Recently, the study of biomedical porous NiTi (SMAs) has attracted much interest in its potential use as a functional material in many engineering and medical applications (Chu *et al.*, 2004), because of their excellent mechanical properties, unique shape memory effect and superelasticity, good corrosion resistance, superior damping capability, and high biocompatibility (Starosvetsky and Gotman., 2001; Kapanen *et al.*, 2001). In addition, the porous NiTi alloy shows promising potential for the application of bone implantation because the porous structure allows the ingrowth of new bone tissue along with the transport of body fluids, thus ensuring a harmonious bond between the implant and the body tissues (Li *et al.*, 2000; Li *et al.*, 2002). Most reports on the preparation of NiTi SMAs by the SHS have focused on obtaining dense NiTi SMAs, whereas less attention has been paid on the preparation of porous NiTi ones. In the present study, the porous feature of SHS products was purposely used to synthesize porous NiTi SMAs. For the fabrication of porous NiTi SMAs by the SHS from the elemental powders, the chemical reaction is weakly exothermic. It is therefore

---

\*Corresponding author.

Email address: sirikul@me.psu.ac.th

necessary to preheat the sample prior to sample ignition to achieve a self-sustained combustion (Tay *et al.*, 2006; Yeh and Sung., 2004; Li *et al.*, 2000). With this mode of combustion, highly porous NiTi alloy at 60% porosity has been produced (Patil *et al.*, 2002). The aim of this work was to study the influences of compaction pressure on the morphology and phase evolution of combustion products.

## 2. Experimental methods of approach

The starting materials used were commercial high-purity powder of Ni (99.8%) and Ti (99.5%) supplied by Alfa Inc., USA. The average particle sizes of Ni and Ti were 16.4  $\mu\text{m}$  and 34.9  $\mu\text{m}$  respectively. The mixed powders of Ni and Ti with equiatomic stoichiometry were blended by a planetary ball mill for 12 hours, and then cold-pressed into a cylindrical sample with a diameter of 14 mm and a height of 28 mm at compaction pressure levels of 8MPa, 16MPa and 64MPa. The powder compact was then loaded into a reaction furnace and heated to 200°C under an argon atmosphere. The preheated compact was ignited at one end by tungsten coil in a furnace. The combustion temperature-time profiles of powder compact were obtained by placing type K thermocouple in a close contact onto the sample surface and the data were recorded using a USB Data Acquisition recorder. The general porosity of the specimens was calculated by the formula

$$\varepsilon = \left( \left[ 1 - \frac{\rho}{\rho_0} \right] \times 100 \right)$$

in which  $\rho$  and  $\rho_0$  are the density of the specimen and its corresponding theoretical density, respectively. The density and the open porosity of the specimen were determined by the liquid weighing method (ASTM B328-73., 1980). The theoretical density value is 6.44 g/cm<sup>3</sup> for the NiTi alloy. After reaction, the microstructural characteristic of products was examined under a scanning electron microscope (SEM). X-ray diffraction (XRD) was used to identify phases.

## 3. Result and Discussion

Figure 1 shows the shape of starting powder observed by SEM. Nickel powders have a spiky surface while titanium powders have an angular shape. Changes in the surface morphologies and the particle size of Ni-Ti powders after ball milling are also shown in Figure 1.

### 3.1 Influence of compaction pressure on the combustion temperature

It can be observed in Figure 2 that the combustion temperature,  $T_c$ , increases with increasing compaction pressure since the higher the compaction pressure, the better the heat transfer from the burned to the unburned region. The maximum combustion temperature in this study is 843°C

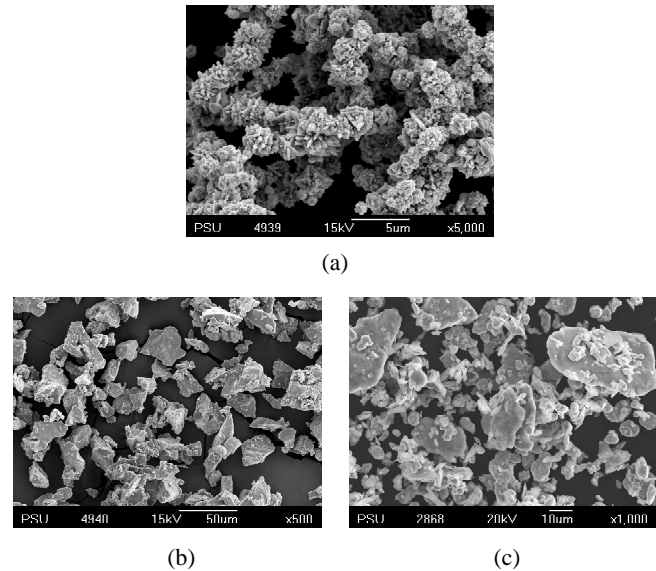


Figure 1. SEM micrograph of (a) Ni powders, (b) Ti powders and (c) Ni-Ti powders after milling for 12 h.

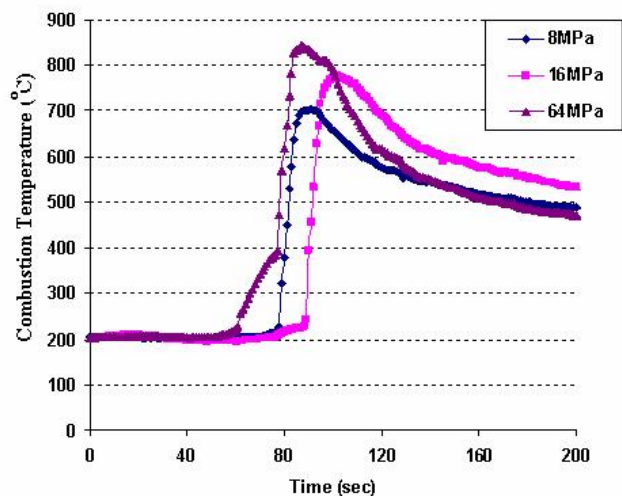


Figure 2. Influence of compaction pressure on combustion temperature of sample compacts at preheating temperature 200°C

at a compaction pressure of 64 MPa. In addition, the highest combustion temperatures of all three samples shown in Figure 2, are below the lowest eutectic temperature (942°C) of the Ni-Ti mixture and below the melting point of the NiTi alloy (1310°C). Therefore, no liquid possibly exists, and solid-state reaction is the dominant mechanism. The original pores in the green compact are hence the main origins of pores obtained in the final products.

### 3.2 Influence of compaction pressure on morphology

Figure 3, the micrographs of porous NiTi SMAs produced by SHS, demonstrates the porous nature of the SHS reacted products. As pointed out by Munir and Wang (1990), pores in SHS-reacted products have five possible

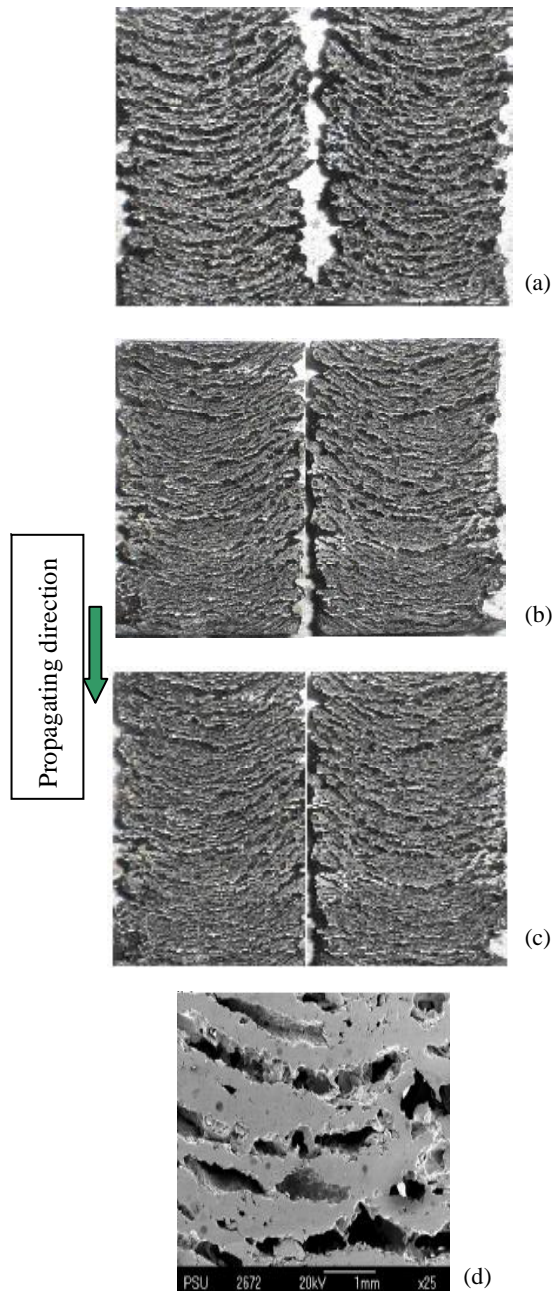


Figure 3. Typical morphology of porous NiTi at different compaction pressure:

- (a) 8MPa, 200°C,
- (b) 16MPa, 200°C,
- (c) 64MPa, 200°C,
- (d) SEM micrographs: 8MPa, 200°C

sources. They are: (1) existing pores in the reactants prior to combustion; (2) differences in molar volume between reactants and products; (3) differences in diffusion rates between nickel and titanium; (4) gas evolution during reaction; and (5) thermal migration due to the high temperature gradient during combustion. Certainly, the first one is the main contribution since the reactants prior to combustion have porosity of 54.8, 44.7 and 35.2 vol.% for the samples compacted at 8, 16 and 64MPa, respectively which are close to the porosity levels of the synthesized products (57.9, 47.7 and 37.4 vol.%), as can be seen in Table 1. Therefore, the porosity level of the samples was effectively reduced by increasing the sample compaction pressure. It is also noted in Table 1 that most pores are interconnected as indicated from the open porosity ratio, which is in excess of 0.88. Porous NiTi SMA with such pore characteristics is suitable for use as hard tissue implants (Chu *et al.*, 2004)

Figures 3a to 3c show a series of longitudinal sections of porous parts produced at various compaction pressures. Although linearly aligned channels in longitudinal sections were observed by Li *et al.* (2000), here we obtained striations in the range of 1 to 4.5 mm long along the transverse direction and perpendicular to the direction of the combustion wavefront during SHS. As shown in Figure 3d, many small pores of near-circular or elliptical shapes were observed by SEM. The cross-sectional views of the porous NiTi samples (Figures 3a-3c) reveal that most pores were interconnected, which is similar to that found in a work by Tay *et al.* (2006). According to Figures 3a-3c, the higher the compaction pressure, the narrower the distance between the adjacent striations and the smaller the pore size. The average measured pore sizes are 497, 441 and 368 mm for the samples compacted at 8, 16 and 64MPa, respectively. This is due to the increase in compaction pressure usually increasing the amount of particle contacts and hence raising the thermal conductivity, the combustion temperature and the heat propagating wave velocity given the stable combustion front to the unburned region.

### 3.3 Influence of compaction pressure on phase evolution

Figure 4 shows an XRD pattern of the reactants. As can be seen, the nickel and titanium powders have been only mechanically mixed without alloying. The XRD patterns of SHS-synthesized porous NiTi SMAs under different compaction pressure are shown in Figure 5. It can be observed from the XRD spectrum in Figure 5 that there is no significant

Table 1. Green porosity, general porosity, open porosity and open porosity ratio at different compaction pressure

Compaction pressure (MPa)	Preheating temperature (°C)	Green porosity (vol.%)	General porosity (vol.%)	Open porosity (vol.%)	Open porosity ratio
8	200	54.8	57.9	55.8	0.96
16	200	44.7	47.7	42.2	0.88
64	200	35.2	37.4	33.8	0.90

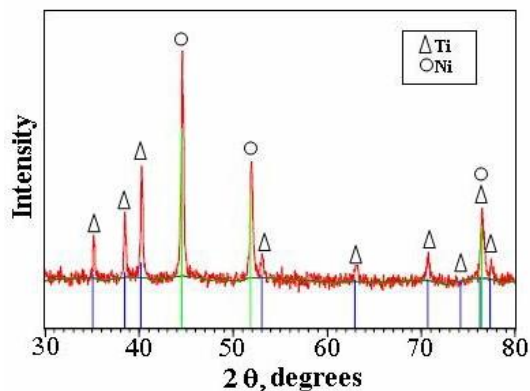


Figure 4. XRD patterns of the Ni-Ti powder mixture

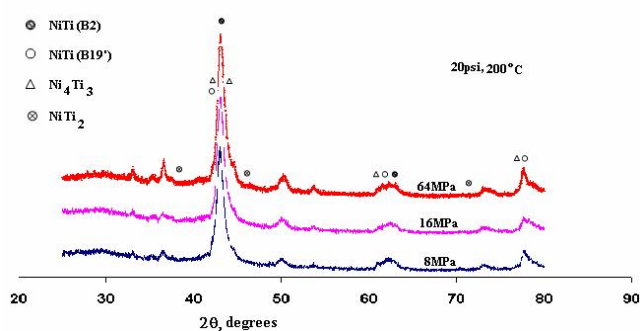


Figure 5. XRD patterns of the SHS-synthesized porous NiTi SMAs with different compaction pressure (8MPa, 16MPa and 64MPa)

ant effect of the compaction pressure on phase evolution and the SHS process results in the formation of several intermetallic compounds, such as NiTi, NiTi<sub>2</sub> and Ni<sub>4</sub>Ti<sub>3</sub>. The B2(NiTi) and B19'(NiTi), which are the desired products, are the predominant phases. The presence of the second phases is the common feature for the products processed by SHS because of the compositional fluctuation in the specimen. This is due to the raw powders being insufficiently mixed and the particle size of the reactants not small enough (Hench and Am., 1991). The presence of the Ni<sub>4</sub>Ti<sub>3</sub> phase observed from the SHS-synthesized porous NiTi (SMAs) can be explained as follows. The overall stoichiometry of the sample was Ni-rich. Moreover, the presence of NiTi<sub>2</sub> as the only second phase could make the parent NiTi phase more Ni-rich (Chu *et al.*, 2004). Among these phases, NiTi and NiTi<sub>2</sub> are the two stable phases, while Ni<sub>4</sub>Ti<sub>3</sub> is a metastable phase observed in Ni-Ti alloys (Li *et al.*; 2000).

#### 4. Conclusions

This study represents an effect of compaction pressure on the morphology and phase evolution of NiTi SMA synthesized by the SHS technique. It was found that not only the porosity level but also the pore structure and pore size are strongly affected by the compaction pressure. With increas-

ing compaction pressure, the porosity level becomes lower and the pore size gets smaller. The average pore size of the synthesized products ranges from 368-497 nm with the total porosity and the open porosity ratio of 37.4-57.9 vol.% and 88-96%, respectively. The primary source of porosity in the synthesized samples was attributed to the sample green porosity. The predominant phases in the porous products are B2(NiTi) and B19'(NiTi) with small amounts of secondary phases, NiTi<sub>2</sub> and Ni<sub>4</sub>Ti<sub>3</sub>. However, there is no influence of the compaction pressure on the formation of phases in the synthesized products.

#### Acknowledgements

This research was sponsored by Graduate Studies Related Research Fund (GSRRF) 2006, and PSU-Revenue Fund 2006. Equipment and facilities were also provided by the Department of Mechanical Engineering and Department of Mining and Materials Engineering, Prince of Songkla University, Hat Yai, Thailand.

#### References

- ASTM Standard B328. 1987. American Society for Testing and Materials, Philadelphia, PA.
- Bertolino, N., Monagheddu, M., Tacca, A., Guiliani, P., Zanotti, C. and Tamburini, U.A. 2003. Ignition Mechanism in Combustion Synthesis of Ti-Al and Ti-Ni Systems. *Intermetallics*. 11, 41-49.
- Chu, C.L., Chung, C.Y., Lin, P.H. and Wang, S.D. 2004. Fabrication of Porous NiTi Shape Memory Alloy for Hard Tissue Implants by Combustion Synthesis. *Materials Science and Engineering A*. 366, 114-119.
- Ganesh, I., Johnson, R., Rao, G.V.N., Mahajan, Y.R., Madavendra, S.S. and Reddy, B.M. 2005. Microwave-Assisted Combustion Synthesis of Nanocrystalline MgAl<sub>2</sub>O<sub>4</sub> Spinel Powder. *Ceramics International*. 31, 67-74.
- Hench, L.L. 1991. Bioceramics: From Concept to Clinic. *Journal of the American Ceramic Society*. 74, 1487-1510.
- Kapanen, A., Ryhanen, J., Danilov, A. and Tuukkanen, J. 2001. Effect of Nickel-Titanium Shape Memory Metal Alloy on Bone Formation. *Biomaterials*. 22 (18), 2475-2480.
- Li, B.Y., Rong, L.J., Li, Y.Y. and Gjunter, V.E. 2000. Synthesis of Porous Ni-Ti Shape Memory Alloys by Self-Propagating High-Temperature Synthesis: Reaction Mechanism and Anisotropy in Pore Structure. *Acta Materialia*. 48, 3895-3904.
- Li, Y.H., Rong, L.J. and Li, Y.Y. 2002. Compressive Property of Porous NiTi Alloy Synthesized by Combustion Synthesis. *Journals of Alloys and Compounds*. 345, 271-274.
- Munir, Z.A. and Wang, L.L. 1990. The Contribution of Thermal Migration to Pore Formation During SHS

- Reactions. *In* Proceedings of First US-Japanese Workshop on Combustion Synthesis, eds Y. Kaieda and J. B. Holt, National Research Institute for Metals. 123-137.
- Patil, K.C., Aruna, S.T. and Mimani, T. 2002. Combustion Synthesis: An Update. *Current Opinion in Solid State Materials Science*. 6, 507-512.
- Starosvetsky, D. and Gotman, I. 2001. Corrosion Behavior of PIRAC nitrided NiTi Shape Memory Surgical Alloy. *Biomaterials*. 22(13), 1853-1859.
- Tay, B.Y., Goh, C.W., Yong, M.S., Soutar, A.M., Li, Q., Ho, M.K., Myint, M.H., Gu, Y.W. and Lim, C.S. 2006. Self-Propagating High-Temperature Synthesis of Porous NiTi. SIMTech technical reports. 7, 21-25.
- Yeh, C.L. and Sung, W.Y. 2004. Synthesis of NiTi Intermetallics by Self-Propagating Combustion. *Journals of Alloys and Compounds*. 376, 79-88.